

rf superconducting quantum interference device metamaterials

N. Lazarides^{a)}

Department of Physics, University of Crete, P.O. Box 2208, 71003 Heraklion, Greece; Institute of Electronic Structure and Laser, Foundation for Research and Technology-Hellas, P.O. Box 1527, 71110 Heraklion, Greece; and Department of Electrical Engineering, Technological Educational Institute of Crete, P.O. Box 140, Stavromenos, 71500, Heraklion, Crete, Greece

G. P. Tsironis

Facultat de Física, Departament d'Estructura i Constituents de la Matèria, Universitat de Barcelona, Av. Diagonal 647, E-08028 Barcelona, Spain; Department of Physics, University of Crete, P.O. Box 2208, 71003 Heraklion, Greece; and Institute of Electronic Structure and Laser, Foundation for Research and Technology-Hellas, P.O. Box 1527, 71110 Heraklion, Greece

(Received 19 January 2007; accepted 13 March 2007; published online 16 April 2007)

A rf superconducting quantum interference device (SQUID) array in an alternating magnetic field is investigated with respect to its effective magnetic permeability, within the effective medium approximation. This system acts as an inherently nonlinear magnetic metamaterial, leading to negative magnetic response, and thus negative permeability above the resonance frequency of the individual SQUIDS. Moreover, the permeability exhibits oscillatory behavior at low field intensities, allowing its tuning by a slight change of the intensity of the applied field. © 2007 American Institute of Physics. [DOI: 10.1063/1.2722682]

A rf superconducting quantum interference device (SQUID) consists of a superconducting ring interrupted by a Josephson junction (JJ).¹ When driven by an alternating magnetic field, the induced supercurrents around the ring are determined by the JJ through the celebrated Josephson relations. This system exhibits rich nonlinear behavior, including chaotic effects.² Recently, quantum rf SQUIDS have attracted great attention, since they constitute essential elements for quantum computing.³ In this direction, rf SQUIDS with one or more zero and/or π ferromagnetic JJs have been constructed.⁴ In this letter we show that rf SQUIDS may serve as constitutive elements for nonlinear magnetic metamaterials (MMs), i.e., artificial, composite, and inherently nonmagnetic media with (positive or negative) magnetic response at microwave frequencies.

Classical MMs are routinely fabricated with regular arrays of split-ring resonators (SRRs), with operating frequencies up to the optical range.⁵ Moreover, MMs with negative magnetic response can be combined with plasmonic wires that exhibit negative permittivity, producing thus left-handed (LH) metamaterials characterized by negative refraction index. Superconducting SRRs promise severe reduction of losses, which constrain the evanescent wave amplification in these materials.⁶ Metamaterials involving superconducting SRRs and/or wires have been recently demonstrated experimentally.⁷ The effect of incorporating superconductors in LH transmission lines has been also studied.⁸ Naturally, the theory of metamaterials has been extended to account for nonlinear effects.^{9–13} Nonlinear MMs support several types of interesting excitations, e.g., magnetic domain walls,¹¹ discrete breathers,¹² and envelope solitons.¹³ Regular arrays of rf SQUIDS offer an alternative for the construction of nonlinear MMs due to the nonlinearity of the JJ.

Very much like the SRR, the rf SQUID [Fig. 1(b)] is a resonant nonlinear oscillator, and similarly it responds in a manner analogous to a magnetic “atom” in a time-varying

magnetic field with appropriate polarization, exhibiting a resonant magnetic response at a particular frequency. The SRRs are equivalently RLC circuits in series, featuring a resistance R , a capacitance C , and an inductance L , working as small dipoles. In turn, adopting the resistively and capacitively shunted junction model for the JJ,¹ the rf SQUIDS are not dipoles but, instead, they feature an inductance L in series with an ideal Josephson element (i.e., for which $I=I_c \sin \phi$, with ϕ the Josephson phase), shunted by a capacitor C and a resistor R [Fig. 1(c)]. However, the fields they produce are approximately those of small dipoles, although quantitatively they are affected by flux quantization in superconducting loops. Consider a rf SQUID with loop area $S=\pi a^2$ (radius a), in a magnetic field of amplitude H_{e0} , frequency ω , and intensity $H_{\text{ext}}=H_{e0} \cos(\omega t)$ perpendicular to its plane (t is the time variable). The field generates a flux $\Phi_{\text{ext}}=\Phi_{e0} \cos(\omega t)$ threading the SQUID loop, with $\Phi_{e0}=\mu_0 S H_{e0}$ and μ_0 the permeability of the vacuum. The flux Φ trapped in the SQUID ring is given (in normalized variables) by

$$f = f_{\text{ext}} + \beta i, \quad (1)$$

where $f=\Phi/\Phi_0$, $f_{\text{ext}}=\Phi_{\text{ext}}/\Phi_0$, $i=I/I_c$, $\beta=\beta_L/2\pi \equiv LI_c/\Phi_0$, I is the current circulating in the ring, I_c is the critical current of the JJ, L is the inductance of the SQUID ring, and Φ_0 is

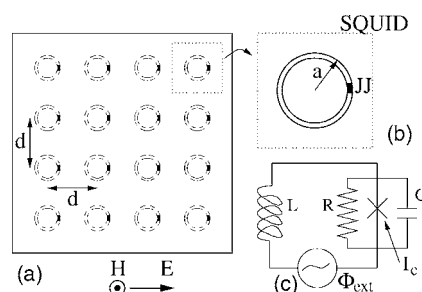


FIG. 1. Schematic drawing of the SQUID array, along with the equivalent circuit for a rf SQUID in external flux Φ_{ext} .

^{a)}Electronic mail: n1@physics.uoc.gr

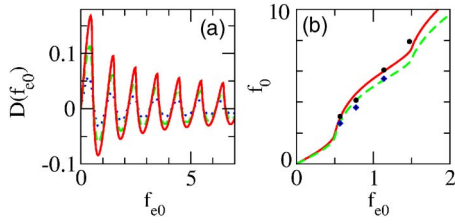


FIG. 2. (Color online) (a) Coefficient D vs the applied flux amplitude f_{e0} , for $\beta=0.15$ (red-solid curve); $\beta=0.10$ (green-dashed curve); $\beta=0.05$ (blue-dotted curve). (b) The amplitude of the flux f_0 vs f_{e0} , for $\Omega=0.9$ (red-solid curve), $\Omega=1.1$ (green-dashed curve), and $\gamma=0.001$, $\beta=0.15$. The black circles and blue diamonds correspond to the numerically obtained f_0 for $\Omega=0.9$ and 1.1 , respectively.

the flux quantum. The dynamics of the normalized flux f is governed by the equation

$$\frac{d^2 f}{d\tau^2} + \gamma \frac{df}{d\tau} + \beta \sin(2\pi f) + f = f_{\text{ext}}, \quad (2)$$

where C and R are the capacitance and resistance, respectively, of the JJ, $\gamma=L\omega_0/R$, $\tau=\omega_0 t$, $\omega_0^2=1/LC$, and

$$f_{\text{ext}} = f_{e0} \cos(\Omega\tau), \quad (3)$$

with $f_{e0}=\Phi_{e0}/\Phi_0$ and $\Omega=\omega/\omega_0$. The small parameter γ actually represents all of the dissipation coupled to the rf SQUID.

An approximate solution for Eq. (2) may be obtained for Ω close to the SQUID resonance frequency ($\Omega \sim 1$) in the nonhysteretic regime $\beta_L < 1$. Following Ref. 14 we expand the nonlinear term in Eq. (2) in a Fourier-Bessel series of the form

$$\beta \sin(2\pi f) = - \sum_{n=1}^{\infty} \frac{(-1)^n}{n\pi} J_n(n\beta_L) \sin(2\pi n f_{\text{ext}}), \quad (4)$$

where J_n is the Bessel function of the first kind, of order n . By substituting Eq. (3) in Eq. (4) and carrying out the Fourier-Bessel expansion of the sine term, one needs to retain only the fundamental Ω component in the expansion.¹⁵ This leads to the simplified expression

$$\beta \sin(2\pi f) \simeq D(f_{e0}) \cos(\Omega\tau), \quad (5)$$

where $D(f_{e0}) = -2 \sum_{n=1}^{\infty} \frac{(-1)^n}{n\pi} J_n(n\beta_L) J_1(2\pi n f_{e0})$. By substitution of Eq. (5) in Eq. (2), the latter can be solved for the flux $f = f_0 \cos(\Omega\tau + \theta)$ in the loop, with

$$f_0 = \frac{f_{e0} - D}{\sqrt{\gamma^2 \Omega^2 + (1 - \Omega^2)^2}}, \quad \theta = \tan^{-1} \left(\frac{-\gamma \Omega}{1 - \Omega^2} \right), \quad (6)$$

where θ is the phase difference between f and f_{ext} . The dependence of D and f_0 on f_{e0} for low field intensity is illustrated in Figs. 2(a) and 2(b), respectively. For larger f_{e0} the coefficient D approaches zero still oscillating, while f_0 approaches a straight line with slope depending on Ω and γ . For $\gamma \ll 1$ and not very close to the resonance, $\theta \approx 0$. It is instructive to express the $\gamma=0$ solution as

$$f = \pm |f_0| \cos(\Omega\tau), \quad |f_0| = (f_{e0} - D) / |1 - \Omega^2|. \quad (7)$$

The plus (minus) sign, corresponding to a phase shift of 0 (π) of f with respect to f_{ext} , is obtained for $\Omega < 1$ ($\Omega > 1$). Thus, the flux f may be either in-phase (+ sign) or in anti-phase (- sign) with f_{ext} , depending on Ω . This is confirmed by numerical integration of Eq. (2), as shown in Fig. 3,

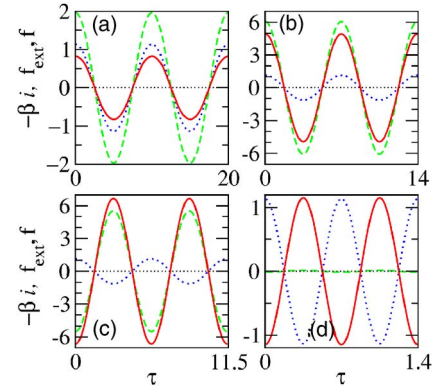


FIG. 3. (Color online) Time dependence of the flux f (green-dashed curves), the applied flux f_{ext} (blue-dotted curves), and the response βi (red-solid curves), for $\beta=0.15$, $\gamma=0.001$, $f_{e0}=1.14$, and (a) $\Omega=0.63$; (b) $\Omega=0.9$; (c) $\Omega=1.1$; (d) $\Omega=9.0$.

where we plot separately the three terms of Eq. (1) in time. The quantities f , f_{ext} , and βi are shown for two periods $T=2\pi/\Omega$ in each case, after they have reached a steady state. For $\Omega < 1$ [Figs. 3(a) and 3(b)], the flux f (green-dashed curves) is in phase with f_{ext} (blue-dotted curves), while for $\Omega > 1$ [Figs. 3(c) and 3(d)] the flux f is in antiphase with f_{ext} . The other curves (red-solid curves) correspond to βi , the response of the SQUID to the applied flux. Away from the resonance, the response is (in absolute value) less than [Fig. 3(a), for $\Omega=0.63$] or nearly equal [Fig. 3(d), for $\Omega=8.98$] to the magnitude of f_{ext} . However, close to resonance, the response βi is much larger than f_{ext} , leading to a much higher flux f [Figs. 3(b) and 3(c) for $\Omega=0.9$ and $\Omega=1.1$, respectively]. Moreover, in Fig. 3(c), f is in antiphase with f_{ext} , showing thus extreme diamagnetic (negative) response. The numerically obtained amplitudes f_0 [depicted as black circles for $\Omega=0.9$ and blue diamonds for $\Omega=1.1$ in Fig. 2(b)] are in fair agreement with the analytical expression, Eq. (6). The agreement becomes better for larger f_{e0} .

We now consider a planar rf SQUID array consisting of identical units [Fig. 1(a)], and forming a lattice of unit-cell side d ; the system is placed in a magnetic field $H_{\text{ext}} \equiv H$ perpendicular to SQUID plane. If the wavelength of H is much larger than d , the array can be treated as an effectively continuous and homogeneous medium. Then, the magnetic induction B in the array plane is

$$B = \mu_0(H + M) \equiv \mu_0 \mu_r H, \quad (8)$$

where $M=SI/d^3$ is the magnetization induced by the current I circulating a SQUID loop and μ_r the relative permeability of the array. Introducing M into Eq. (8) and using Eqs. (1), (2), and (7), we get

$$\mu_r = 1 + \tilde{F}(\pm |f_0|/f_{e0} - 1), \quad (9)$$

where $\tilde{F} = \pi^2(\mu_0 a/L)(a/d)^3$. The coefficient \tilde{F} has to be very small ($\tilde{F} \ll 1$), so that magnetic interactions between individual SQUIDs can be neglected in a first approximation. Recall that the plus sign in front of $|f_0|/f_{e0}$ should be taken for $\Omega < 1$, while the minus sign should be taken for $\Omega > 1$. In Fig. 4 we plot μ_r both for $\Omega < 1$ [Fig. 4(a)] and $\Omega > 1$ [Fig. 4(b)], for three different values of \tilde{F} . In real arrays, that coefficient could be engineered to attain the desired value. In both Figs. 4(a) and 4(b), the relative permeability μ_r oscillates for low intensity fields (low f_{ext}), while it tends to a

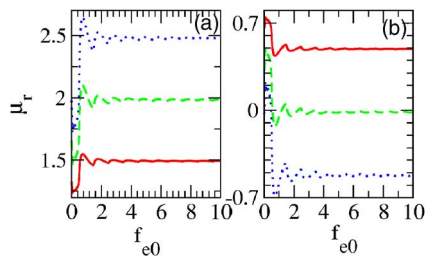


FIG. 4. (Color online) Relative permeability μ_r vs f_{e0} , for $\tilde{F}=0.01$ (red-solid curves), $\tilde{F}=0.02$ (green-dashed curves), $\tilde{F}=0.03$ (blue-dotted curves), and (a) $\Omega=0.99$; (b) 1.01.

constant at larger f_{ext} . In Fig. 4(a) ($\Omega < 1$), the relative permeability μ_r is always positive, while it increases with increasing \tilde{F} . In Fig. 3(b), however, μ_r may assume both positive and negative values, depending on the value of \tilde{F} . With appropriate choice of \tilde{F} , it becomes oscillatory around zero [green-dashed curve in Fig. 4(b)], allowing tuning from positive to negative μ_r with a slight change of f_{ext} .

In conclusion, we have shown that a planar rf SQUID array exhibits large magnetic response close to resonance, which may be negative above the resonance frequency, leading to effectively negative μ_r . For low field intensities (low f_{ext}), μ_r exhibits oscillatory behavior which gradually disappears for higher f_{ext} . This behavior may be exploited to construct a flux-controlled metamaterial (as opposed to voltage-controlled metamaterial demonstrated in Ref. 16). The physical parameters required for the rf SQUIDs giving the dimensionless parameters used above are not especially formidable. A rf SQUID with $L \approx 105$ pH, $C \approx 80$ fF, and $I_c \approx 3$ μ A, would give $\beta \approx 0.15$ ($\beta_L \approx 0.94$). For these parameters, a value of the resistance $R \approx 3.6$ k Ω is required in order to have $\gamma \approx 10^{-3}$, used in the numerical integration of Eq. (2). However, our results are qualitatively valid for γ even an order of magnitude larger, in which case $R \approx 360$ Ω . We note that $\omega_0 = \omega_p / \sqrt{\beta_L}$, where ω_p is the plasma frequency of the JJ. For the parameters considered above, where β_L is slightly less than unity, the frequencies ω_0 and ω_p are of the same order. However, ω_p does not seem to have any special role in the microwave response of the rf

SQUID. Du *et al.* have studied the quantum version of a SQUID array as a LH metamaterial, concluded that negative refractive index with low loss may be obtained in the quantum regime.¹⁷ Consequently, μ_r can be negative at some specific frequency range. However, their corresponding expression for μ_r is linear, i.e., it does not depend on the amplitude of the applied flux, and thus it does not allow flux tuning. Moreover, experiments with SQUID arrays in the quantum regime, where individual SQUIDs can be described as two-level systems, are much more difficult to realize.

The authors acknowledge support from the grant ‘‘Pythagoras II’’ (KA. 2102/TDY 25) of the Greek Ministry of Education and the European Union and Grant No. 2006PIV10007 of the Generalitat de Catalunya, Spain.

- ¹K. K. Likharev, *Dynamics of Josephson Junctions and Circuits* (Gordon and Breach, Philadelphia, 1986).
- ²K. Fesser, A. R. Bishop, and P. Kumar, Appl. Phys. Lett. **43**, 123 (1983).
- ³M. F. Bocko, A. M. Herr, and M. J. Feldman, IEEE Trans. Appl. Supercond. **7**, 3638 (1997).
- ⁴T. Yamashita, S. Takahashi, and S. Maekawa, Appl. Phys. Lett. **88**, 132501 (2006).
- ⁵T. J. Yen, W. J. Padilla, N. Fang, D. C. Vier, D. R. Smith, J. B. Pendry, D. N. Basov, and X. Zhang, Science **303**, 1494 (2004).
- ⁶M. C. Ricci, H. Xu, S. M. Anlage, R. Prozorov, A. P. Zhuravel, and A. V. Ustinov, IEEE Trans. Appl. Supercond. (to be published), e-print cond-mat/0608737.
- ⁷M. C. Ricci, N. Orloff, and S. M. Anlage, Appl. Phys. Lett. **87**, 034102 (2005).
- ⁸H. Salehi, A. H. Majedi, and R. R. Mansour, IEEE Trans. Appl. Supercond. **15**, 996 (2005).
- ⁹A. A. Zharov, I. V. Shadrivov, and Y. Kivshar, Phys. Rev. Lett. **91**, 037401 (2003); M. Lapine, M. Gorkunov, and K. H. Ringhofer, Phys. Rev. E **67**, 065601 (2003).
- ¹⁰N. Lazarides and G. P. Tsironis, Phys. Rev. E **71**, 036614 (2005); I. Kourakis and P. K. Shukla, *ibid.* **72**, 016626 (2005).
- ¹¹I. V. Shadrivov, A. A. Zharov, N. A. Zharova, and Y. S. Kivshar, Photonics Nanostruct. Fundam. Appl. **4**, 69 (2006).
- ¹²N. Lazarides, M. Eleftheriou, and G. P. Tsironis, Phys. Rev. Lett. **97**, 157406 (2006).
- ¹³I. Kourakis, N. Lazarides, and G. P. Tsironis, e-print cond-mat/0612615.
- ¹⁴S. N. Ermé, H.-D. Hahlbohm, and H. Lübbig, J. Appl. Phys. **47**, 5440 (1976).
- ¹⁵A. R. Bulsara, J. Appl. Phys. **60**, 2462 (1986).
- ¹⁶O. Reynet and O. Acher, Appl. Phys. Lett. **84**, 1198 (2004).
- ¹⁷C. Du, H. Chen, and S. Li, Phys. Rev. B **74**, 113105 (2006).